Heterozygous mutation of ataxia-telangiectasia mutated gene aggravates hypercholesterolemia in apoE-deficient mice

DongFang Wu,[1,2,*] Hong Yang,[1,†] Wei Xiang,[*] LiChun Zhou,[*] MingJian Shi,[*] George Julies,[†] Janice M. LaPlante,[§] Billy R. Ballard,[*] and ZhongMao Guo[3,*]

Department of Pathology, Anatomy, and Cell Biology* and Department of Physiology,† Meharry Medical College, Nashville, TN 37208; and Division of Endocrinology, Diabetes, and Hypertension,§ Brigham and Women's Hospital, Harvard Medical School, Boston, MA 02115

Abstract **Individuals with a heterozygous mutation at the ataxia-telangiectasia mutated gene (*ATM*) have been reported to be predisposed to ischemic heart disease. This report examined for the first time the effect of a heterozygous *ATM* mutation ($ATM^{+/-}$) on plasma lipid levels and atherosclerosis intensity using $ATM^{+/-}$, $ATM^{+/+}$ (wild type), $ATM^{+/+}/LDLR^{-/-}$ (low density lipoprotein receptor knockout), $ATM^{+/-}/LDLR^{-/-}$, $ATM^{+/+}/ApoE^{-/-}$ (apolipoprotein E knockout), and $ATM^{+/-}/ApoE^{-/-}$ mice. Our data demonstrated that the plasma cholesterol and triglyceride levels in $ATM^{+/-}$ and $ATM^{+/-}/LDLR^{-/-}$ mice were approximately the same as those in $ATM^{+/+}$ and $ATM^{+/+}/LDLR^{-/-}$ control mice, respectively. In contrast, the plasma cholesterol level was significantly higher in $ATM^{+/-}/ApoE^{-/-}$ mice than in $ATM^{+/+}/ApoE^{-/-}$ control mice. In addition, the $ATM^{+/-}/ApoE^{-/-}$ mice showed higher plasma apoB-48 levels, slower clearance for plasma apoB-48-carrying lipoproteins, and more advanced atherosclerotic lesions in the aorta compared with the $ATM^{+/+}/ApoE^{-/-}$ mice. These novel results suggest that the product of *ATM* is involved in an apoE-independent pathway for catabolism of apoB-48-carrying remnants; therefore, superimposition of a heterozygous *ATM* mutation onto an *ApoE* deficiency background reduces the clearance of apoB-48-carrying lipoproteins from the blood circulation and promotes the formation of atherosclerosis.**—Wu, D., H. Yang, W. Xiang, L. Zhou, M. Shi, G. Julies, J. M. LaPlante, B. R. Ballard, and Z. Guo. **Heterozygous mutation of ataxia-telangiectasia mutated gene aggravates hypercholesterolemia in apoE-deficient mice. *J. Lipid Res.* 2005.** 46: **1380–1387.**

Supplementary key words apolipoprotein E • apolipoprotein B-48-carrying lipoprotein • cholesterol • atherosclerosis

The product of the ataxia-telangiectasia mutated gene (*ATM*) has been reported to be a nuclear protein and involved in several signaling pathways, including DNA damage recognition, cell cycle control, and meiotic recombination (for review, see 1). It is now known that a fraction of ATM is also present in the cytoplasm and associated with vesicular structures such as peroxisomes (2). Ataxia-telangiectasia patients [i.e., those individuals carrying mutations at both *ATM* alleles ($ATM^{-/-}$)] express a variety of progressive clinical symptoms, such as cerebellar ataxia, telangiectasias, and a high incidence of cancer (for review, see 3). Cells obtained from ataxia-telangiectasia patients are more sensitive to ionizing radiation and show increased chromosomal aberrations compared with those obtained from normal subjects (4). Individuals with an *ATM* mutation in one allele ($ATM^{+/-}$) are spared most of the symptoms of the disease but are predisposed to cancer (5). A close review of the literature suggests that heterozygous *ATM* deficiency might also increase the risk of atherosclerosis-related cardiovascular diseases. For example, Swift and Chase (6) reported that the age-related mortality of heterozygous *ATM* carriers was increased markedly compared with the general population and that ischemic heart disease was one of the underlying causes for the early death of these individuals. Ataxia-telangiectasia patients reportedly have increased plasma cholesterol and triglyceride levels (7), which are the two major risk factors for atherosclerosis. However, ataxia-telangiectasia patients do not usually live past 20 or 30 years of age, and atherosclerosis has not been studied in these individuals.

More recently, a mouse model in which the *ATM* gene

Manuscript received 28 October 2004 and in revised form 31 March 2005.

Published, JLR Papers in Press, May 1, 2005.
DOI 10.1194/jlr.M400430-JLR200

Abbreviations: apoE, apolipoprotein E; *ATM*, ataxia-telangiectasia mutated gene; FPLC, fast-performance liquid chromatography; LDLR, low density lipoprotein receptor; LRP, LDLR-related protein.

[1] D. Wu and H. Yang contributed equally to this work.

[2] Present address of D. Wu: The Renmin Hospital of Wuhan University, Wuhan City, Hubei 430060, People's Republic of China.

[3] To whom correspondence should be addressed.
e-mail: zguo@mmc.edu

had a truncated mutation in the region of the commonly affected gene site in many ataxia-telangiectasia patients has been generated by Barlow et al. (8). Mice with the homozygous *ATM* mutation ($ATM^{-/-}$) demonstrate many characteristics common in the human ataxia-telangiectasia population, such as growth retardation, neurological dysfunction, and lymphocyte maturation defects (8). Fibroblasts from $ATM^{-/-}$ mice display a higher level of double-strand breaks and chromosomal aberrations than those obtained from wild-type ($ATM^{+/+}$) mice (9). Mice with the heterozygous *ATM* mutation ($ATM^{+/-}$) appear healthy. Similar to human $ATM^{+/-}$ subjects, $ATM^{+/-}$ mice are spared most of the symptoms of the disease but are predisposed to cancer (5). In addition, $ATM^{+/-}$ mice show a greater sensitivity to irradiation-induced cataracts (10) and radiation oncogenesis (11) compared with $ATM^{+/+}$ controls.

In this report, we studied the effects of a heterozygous *ATM* mutation on plasma lipid levels and atherosclerosis intensity using $ATM^{+/-}$ mice. By cross-breeding the $ATM^{+/-}$ mice with mice lacking both apolipoprotein E ($ApoE^{-/-}$) alleles or with mice lacking both low density lipoprotein receptor ($LDLR^{-/-}$) alleles, we obtained the following four inbred lines: *1)* mice with a heterozygous mutation in *ATM* and homozygous mutations in *ApoE* ($ATM^{+/-}/ApoE^{-/-}$); *2)* mice with intact *ATM* and homozygous mutations in *ApoE* ($ATM^{+/+}/ApoE^{-/-}$); *3)* mice with a heterozygous mutation in *ATM* and homozygous mutations in *LDLR* ($ATM^{+/-}/LDLR^{-/-}$); and *4)* mice with intact *ATM* and homozygous mutations in *LDLR* ($ATM^{+/+}/LDLR^{-/-}$). It has been reported that the $ApoE^{-/-}$ mice have 4- to 5-fold higher plasma cholesterol than wild-type mice and develop widespread atherosclerosis at vascular sites typically affected in human atherosclerosis (12). The $LDLR^{-/-}$ mice have ~2-fold more plasma cholesterol than do wild-type mice; however, they exhibit massive increases in plasma cholesterol and develop atherosclerosis throughout the aorta in response to a high-fat diet (13). In the present study, we observed that the plasma cholesterol levels among the $ATM^{+/-}$ and $ATM^{+/-}/LDLR^{-/-}$ mice were approximately the same as those seen among the $ATM^{+/+}$ and $ATM^{+/+}/LDLR^{-/-}$ controls, respectively. However, the $ATM^{+/-}/ApoE^{-/-}$ mice showed increased plasma cholesterol levels and more advanced atherosclerotic lesions compared with their $ATM^{+/+}/ApoE^{-/-}$ littermates. Moreover, $ATM^{+/-}/ApoE^{-/-}$ mice showed increased plasma apoB-48 and reduced clearance for apoB-48-carrying lipoproteins. These results indicate that, in the background of an *ApoE* deficiency, a heterozygous mutation at *ATM* reduces the removal of plasma apoB-48-carrying lipoproteins, resulting in severe hypercholesterolemia and atherosclerosis.

MATERIALS AND METHODS

Animals

The *ATM* mutation mice were kindly provided by Dr. Anthony Wynshaw-Boris (University of California, San Diego, CA). These mice were generated with a 129vEv genetic background (8) and were backcrossed into C57BL/6 for 12 generations. $ApoE^{-/-}$, $LDLR^{-/-}$, and $ApoB^{48/48}/ApoE^{-/-}$ mice were obtained from the Jackson Laboratory (Bar Harbor, ME). $ApoE^{-/-}$ mice were generated by Piedrahita et al. (12) and were backcrossed to C57BL/6 for more than 10 generations. $LDLR^{-/-}$ mice were generated by Ishibashi et al. (13) and were backcrossed to C57BL/6 for more than five generations. $ApoB^{48/48}/ApoE^{-/-}$ mice were obtained by crossbreeding $ApoE^{-/-}$ mice with $ApoB^{48/48}$ mice. The $ApoB^{48/48}$ mice were generated by Farese et al. (14). These mice expressed only apoB-48 and not apoB-100. The mice deficient in both *ATM* and *ApoE* were obtained by crossbreeding $ATM^{+/-}$ and $ApoE^{-/-}$ mice. The mice deficient in both *ATM* and *LDLR* genes were obtained by crossbreeding $ATM^{+/-}$ and $LDLR^{-/-}$ mice. In the present study, $ATM^{+/-}$, $ATM^{+/-}/ApoE^{-/-}$, and $ATM^{+/-}/LDLR^{-/-}$ mice were used at 14 weeks of age. These mice appeared as healthy as their $ATM^{+/+}$, $ATM^{+/+}/ApoE^{-/-}$, and $ATM^{+/+}/LDLR^{-/-}$ littermates. $ATM^{+/-}/ApoE^{-/-}$ mice and their $ATM^{+/+}/ApoE^{-/-}$ controls were fed a chow diet containing ~5% fat and 19% protein by weight (Harlan Teklad, Madison, WI) after weaning. From 6 weeks of age, the $ATM^{+/-}$ and $ATM^{+/-}/LDLR^{-/-}$ mice and their $ATM^{+/+}$ and $ATM^{+/+}/LDLR^{-/-}$ littermates were fed either normal chow or a high-fat diet containing 15% fat and 1.25% cholesterol by weight (Harlan Teklad) for 8 weeks. All procedures for handling the animals were approved by the Institutional Animal Care and Use Committees of Meharry Medical College and were performed in accordance with the guidelines of the American Association for Accreditation of Laboratory Animal Care and the National Institutes of Health.

Analysis of plasma and lipoprotein lipids

Approximately 0.5 ml of blood was collected from the posterior vena cava of mice anesthetized with an analgesic cocktail as described previously (15). A 100 μl plasma sample obtained from individual mice was fractionated using fast-performance liquid chromatography (FPLC) (Äkta FPLC 900; Amersham Biosciences, Piscataway, NJ) in a buffer containing 0.15 M NaCl, 0.01 M Na_2HPO_4, and 0.1 mM EDTA, pH 7.5, at a flow rate of 0.5 ml/min. Forty fractions (0.5 ml/fraction) were collected. The levels of triglycerides, phospholipids, total cholesterol, and free cholesterol in the plasma and FPLC fractions were measured by spectrophotometric quantification using reagents obtained from Sigma Chemical Co. (St. Louis, MO) and Wako Chemicals USA (Richmond, VA). Briefly, aliquoted plasma and FPLC fractions were mixed with triglyceride, phophospholipid, or cholesterol reaction reagents on a glass microplate. These mixtures were incubated at 37°C for 10 min. The absorbance spectra were read using a Dynex microplate reader (Thermo Labsystems, Franklin, MA) with the wavelength as described by the manufacturer. Lipid concentrations were determined based on the absorbance obtained by incubation of the triglyceride, phospholipid, and cholesterol standards provided by Sigma and Wako. The lipid contents in various lipoproteins were calculated from the concentrations in the FPLC fractions as described by Hasty et al. (16). Fractions 14–17 contained VLDL and chylomicrons, fractions 18–25 contained LDL, and fractions 26–40 contained HDL.

SDS-PAGE

A 0.4 ml sample of mouse plasma was overlaid with 0.6 ml of a KBr gradient solution (d = 1.215). Total lipoproteins were isolated from these samples using a Sorvall Discovery M150 ultracentrifuge (Kendro Laboratory Products, Asheville, NC) at 120,000 rpm for 2 h. Lipoproteins from two centrifuge tubes were pooled and delipidated with ethyl ether as described by Mindham and Mayes (17). The apolipoprotein extracts (50 μg) were boiled for 3 min in a sampling buffer containing 125 mM Tris-HCl, 20% glycerol, 4% SDS, 0.05% bromophenol blue, and 4% 2-mercap-

toethanol. The resulting samples were electrophoresed on a SDS-5%/15% polyacrylamide gradient gel. Proteins were stained with Coomassie blue. The gel images were captured with an AlphaImager analysis system (Alpha Innotech Co., San Leandro, CA), and the relative intensity of the apoB-48 band was quantified using the AlphaImager analysis system density analysis software.

ApoB-48-carrying lipoprotein clearance

ApoB-48-carrying lipoproteins were prepared from the plasma of $ApoB^{48/48}/ApoE^{-/-}$ mice. Plasma was overlaid with a KBr gradient solution ($d < 1.006$) and centrifuged at 120,000 rpm for 2 h with a Sorvall Discovery M150 ultracentrifuge. The apoB-48-carrying lipoproteins were collected, dialyzed in PBS (pH 7.4) containing 10 mM EDTA for 48 h at 4°C, and filtered through a 0.45 μm filter. One milliliter of apoB-48-carrying lipoproteins at a concentration of 1 mg/ml was mixed with 0.2 ml of 1 M glycine buffer in 0.25 M NaOH (pH 10) and then mixed with a solution containing 7 μl of 100 mM iodine monochloride, 7 μl of 100 μCi/μl ^{125}I, and 25 μl of 1 M glycine buffer in 0.25 M NaOH (pH 10). The reaction mixture was incubated at room temperature for 10 min and then applied to a 10 DG chromatography column (Bio-Rad Laboratories, Hercules, CA) to remove free iodine (18). The ^{125}I-labeled apoB-48-carrying lipoproteins were eluted with PBS (pH 7.4) and dialyzed extensively against PBS (pH 7.4). The radiolabeled apoB-48-carrying lipoproteins (1.5 μg protein/4 μl/g body weight) were injected into the tail vein of the $ATM^{+/-}/ApoE^{-/-}$ and $ATM^{+/+}/ApoE^{-/-}$ mice. Blood (25 μl) was drawn by retro-orbital venous plexus puncture at the indicated time points after injection. Aliquots of plasma were analyzed for radioactivity on a universal γ counter (1282 Compugamma; Perkin-Elmer Life and Analytic Science, Shelton, CT). Total counts in the plasma were calculated assuming that plasma represents 4% (v/w) of body weight. After the last blood sampling procedure, the mice were flush-perfused with PBS. Whole livers were collected, and the radioactivity in the liver was determined.

Hepatic triglyceride and apoB-100 secretion

Fasted mice were placed on fat-free food for 2 h and then injected via tail vein with 200 μl of 10% Triton WR1339 solution (Sigma). Blood (40 μl) was drawn by retro-orbital venous plexus puncture before and after the Triton injection at the indicated times. Plasma triglycerides were measured with spectrophotometric quantification as described above. The presence and quantity of apoB-100 was determined with Western blots. Briefly, 3 μl of plasma was separated on a 6% SDS-PAGE gel, and proteins were transferred to nitrocellulose membranes electrophoretically using a semidry transfer system (Bio-Rad Laboratories). The membrane was immunoblotted sequentially with an apoB antibody (Santa Cruz Biotechnology, Santa Cruz, CA) and a horseradish peroxidase-conjugated secondary antibody. After incubation with an ECL plus Western blotting detection system (Amersham Biosciences, Piscataway, NJ), protein fluorescence on the membrane was detected with a laser scanner (Typhoon 9410; Amersham Biosciences), and the fluorescence intensity of apoB-100 was quantified with an image-analysis system (ImageQuant; Amersham Biosciences).

Quantification of atherosclerotic lesions in the aorta

Under anesthesia, the mice were perfusion-fixed with 4% paraformaldehyde containing 20 μM butylated hydroxytoluene and 2 μM EDTA at a constant, near-physiological pressure (80 mm Hg) (15). After fixation, the heart and the aorta tree were removed from the body. The aorta was cut at 2 mm from the heart. The proximal aorta attached with the heart was used to prepare microscope sections as described previously (15). Briefly, the heart was transversely sectioned immediately below and parallel with a plane formed by drawing a line between the atrial leaflets. The lower section of the heart was discarded, and the portion with the attached aorta was placed on a metal stub using optimal cutting temperature compound (Sakura Finetek USA, Torrance, CA) such that sectioning followed the line from the attached aorta toward the aorta root where the aortic valves were attached. Sections (8 μm) were cut from the site where the aorta valve cups emerge from the aorta root. Every other section was collected onto a set of microscope slides and stained with Oil Red O (Sigma). The slides were viewed with a microscope (E600; Nikon Instruments, Inc., Melville, NY) equipped with a color digital camera (CoolSnaps; Nikon Instruments) and a computer image-acquisition system (MetaMorph image system; Nikon Instruments). The average area (μm^2) and morphological features (foam cell deposition, cholesterol clefts, acellular areas, and fibrous caps) of the lesions in 16 sections were determined for each mouse (15). The distal aorta (2 mm from the heart to the iliac bifurcation) was opened longitudinally using microscissors and pinned flat on a black wax surface in a dissecting pan on a dissecting microscope (SMZ1000; Nikon Instruments). The en face preparation was fixed overnight and stained with Sudan IV (Sigma). The photo-image of the aorta was captured with a CoolSnaps digital camera (Nikon Instruments) mounted on the SMZ1000 dissecting microscope. The total aortic area and the atherosclerotic lesion area were measured using the MetaMorph image system (Nikon Instruments). Data were expressed as percentages of the aortic surface area covered by atherosclerotic lesions. All measurements were conducted in a double-blind manner (i.e., the person taking the measurements was not aware of the tissue sources, and animals associated with each tissue sample were identified only when all of the tissues had been analyzed).

Statistical analysis

The data are reported as means ± SEM. The differences between $ATM^{+/-}$ and $ATM^{+/+}$ mice, between $ATM^{+/-}/ApoE^{-/-}$ and $ATM^{+/+}/ApoE^{-/-}$ mice, and between $ATM^{+/-}/LDLR^{-/-}$ and $ATM^{+/+}/LDLR^{-/-}$ mice fed normal chow or a high-fat diet were analyzed by multiple-factor ANOVA followed by a Shapiro-Wilk test. Differences were considered significant at $P < 0.05$. All statistical analyses were performed with STASTIX software (Analytical Software, Tallahassee, FL).

RESULTS

Plasma and lipoprotein lipids

Table 1 shows plasma and lipoprotein lipids in $ATM^{+/+}/ApoE^{-/-}$ and $ATM^{+/-}/ApoE^{-/-}$ mice fed a normal chow diet. The plasma levels of total, free, and esterified cholesterol in the $ATM^{+/-}/ApoE^{-/-}$ mice were significantly higher than those determined for their $ATM^{+/+}/ApoE^{-/-}$ littermates. The ratio of esterified cholesterol to total cholesterol, however, was indistinguishable in the $ATM^{+/+}/ApoE^{-/-}$ and $ATM^{+/-}/ApoE^{-/-}$ mice, with ~60% of the plasma cholesterol being esterified. To investigate the distribution of cholesterol among the lipoproteins, mouse plasma was fractionated with a FPLC system. As shown in **Fig. 1**, the severe hypercholesterolemia of the $ATM^{+/-}/ApoE^{-/-}$ mice arose mainly from increased cholesterol levels in the VLDL and LDL fractions. The mean levels of total, free, and esterified cholesterol in the VLDL and LDL fractions were significantly higher in the $ATM^{+/-}/ApoE^{-/-}$ mice than in the $ATM^{+/+}/ApoE^{-/-}$ mice (Table 1). In con-

TABLE 1. Lipid concentrations in mouse plasma and lipoproteins

Source	Total Cholesterol	Free Cholesterol	Esterified Cholesterol	Phospholipid	Triglyceride
$ATM^{+/+}/ApoE^{-/-}$					
Plasma	486 ± 29	196 ± 15	314 ± 20	324 ± 18	146 ± 18
VLDL	304 ± 23	140 ± 8	189 ± 13	159 ± 11	95 ± 12
LDL	139 ± 16	48 ± 7	89 ± 6	97 ± 12	22 ± 6
HDL	47 ± 6	13 ± 4	37 ± 5	72 ± 9	12 ± 5
$ATM^{+/-}/ApoE^{-/-}$					
Plasma	652 ± 33[a]	276 ± 17[a]	405 ± 25[a]	395 ± 22[a]	162 ± 32
VLDL	416 ± 18[a]	197 ± 13[a]	237 ± 10[a]	201 ± 14[a]	115 ± 18
LDL	177 ± 14[a]	72 ± 6[a]	113 ± 8[a]	115 ± 12	31 ± 11
HDL	57 ± 7	14 ± 4	44 ± 6	78 ± 14	14 ± 7

Plasma was obtained from $ATM^{+/-}/ApoE^{-/-}$ and $ATM^{+/+}/ApoE^{-/-}$ mice and lipoproteins were fractionated using a fast-performance liquid chromatography (FPLC) system as described in Materials and Methods. Total cholesterol, free cholesterol, phospholipid, and triglyceride in the plasma and FPLC fractions containing VLDL, LDL, and HDL were determined as described in Materials and Methods. Esterified cholesterol was calculated as the difference between total cholesterol and free cholesterol. Values shown are mg/dl and represent means ± SEM of 15 mice.

[a] Significantly different from $ATM^{+/+}/ApoE^{-/-}$ mice ($P < 0.05$).

trast, the cholesterol levels in the HDL fraction were comparable between the $ATM^{+/+}/ApoE^{-/-}$ and $ATM^{+/-}/ApoE^{-/-}$ mice (Table 1). The $ATM^{+/-}/ApoE^{-/-}$ mice also showed significantly increased plasma phospholipid levels compared with the $ATM^{+/+}/ApoE^{-/-}$ mice. The plasma triglyceride level in the $ATM^{+/-}/ApoE^{-/-}$ mice was slightly, but not significantly, higher than that in $ATM^{+/+}/ApoE^{-/-}$ mice.

We also quantified the apolipoprotein levels in the mouse plasma with SDS-PAGE. Whereas apoB-48 and apoB-100 were barely detectable in the wild-type mice, apoB-48 was increased in both the $ATM^{+/+}/ApoE^{-/-}$ and $ATM^{+/-}/ApoE^{-/-}$ mice, with the greatest change seen in the $ATM^{+/-}/ApoE^{-/-}$ mice. As shown in **Fig. 2**, the level of apoB-48 in $ATM^{+/-}/ApoE^{-/-}$ mice was ~30% higher than that in the $ATM^{+/+}/ApoE^{-/-}$ mice. In contrast to the changes in apoB-48, the levels of apoB-100 in $ATM^{+/-}/ApoE^{-/-}$ and $ATM^{+/+}/ApoE^{-/-}$ mice were comparable (Fig. 2). These data suggest that the increased plasma lipids observed in the $ATM^{+/-}/ApoE^{-/-}$ mice mainly result from an increase in the plasma apoB-48-carrying lipoproteins.

Table 2 compares the plasma cholesterol and triglyceride levels between $ATM^{+/-}$ mice and their $ATM^{+/+}$ littermates and between $ATM^{+/-}/LDLR^{-/-}$ mice and their $ATM^{+/+}/LDLR^{-/-}$ littermates fed normal chow or a high-fat diet. Feeding the mice the high-fat diet increased the plasma cholesterol content in the $ATM^{+/-}$ and $ATM^{+/+}$ mice but did not increase the plasma triglycerides. In contrast, this high-fat diet increased both cholesterol and triglyceride levels in the $ATM^{+/-}/LDLR^{-/-}$ and $ATM^{+/+}/LDLR^{-/-}$ mice. However, the plasma cholesterol and triglyceride levels in the $ATM^{+/-}$ and $ATM^{+/-}/LDLR^{-/-}$ mice were comparable with those in the $ATM^{+/+}$ and

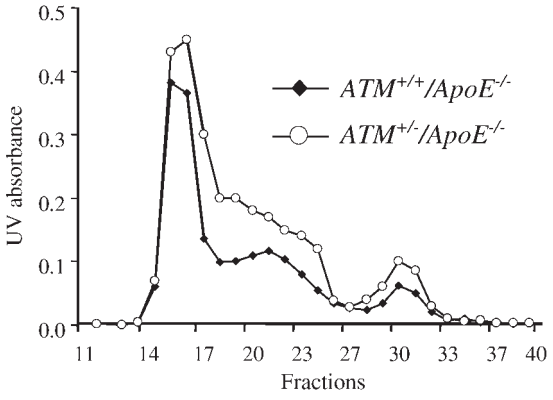

Fig. 1. Fast-performance liquid chromatography (FPLC) profile of plasma cholesterol. Plasma obtained from $ATM^{+/-}/ApoE^{-/-}$ and $ATM^{+/+}/ApoE^{-/-}$ mice was fractionated with a FPLC system. The cholesterol level in FPLC fractions was measured as described in Materials and Methods. UV, ultraviolet.

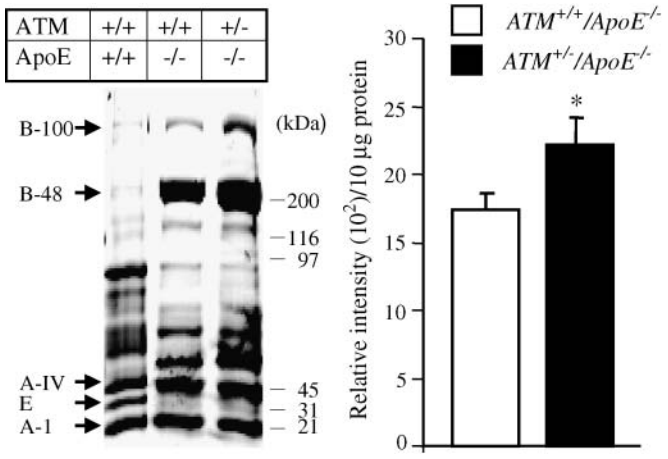

Fig. 2. SDS-PAGE of apolipoproteins. Total lipoproteins ($d < 1.215$) were isolated by ultracentrifugation. The delipidated apolipoproteins were subjected to electrophoresis on a 5–15% SDS-polyacrylamide gradient gel and stained with Coomassie blue. The left panel shows a representative gel. The migration positions of apolipoproteins are denoted. The right panel compares the level of apoB-48 in the plasma of $ATM^{+/-}/ApoE^{-/-}$ and $ATM^{+/+}/ApoE^{-/-}$ mice. Values represent means ± SEM of four separate experiments in which plasma was pooled from two mice. * Significantly different from $ATM^{+/+}/ApoE^{-/-}$ mice ($P < 0.05$).

TABLE 2. Cholesterol and triglyceride concentrations in mouse plasma

Mouse	Normal Chow		High-Fat Diet	
	Total Cholesterol	Triglyceride	Total Cholesterol	Triglyceride
$ATM^{+/+}$	105 ± 5	60 ± 9	174 ± 16[a]	57 ± 5
$ATM^{+/-}$	109 ± 9	72 ± 8	192 ± 14[a]	63 ± 5
$ATM^{+/+}/LDLR^{-/-}$	263 ± 16	158 ± 17	922 ± 81[a]	342 ± 61[a]
$ATM^{+/-}/LDLR^{-/-}$	274 ± 25	143 ± 12	905 ± 58[a]	355 ± 30[a]

$ATM^{+/-}$ mice and their $ATM^{+/+}$ littermates and $ATM^{+/-}/LDLR^{-/-}$ mice and their $ATM^{+/+}/LDLR^{-/-}$ littermates were fed normal chow or high-fat diet. Blood samples were collected after overnight fasting. Plasma total cholesterol and triglycerides were determined as described in Materials and Methods. Values shown are mg/dl and represent means ± SEM of 15 mice.

[a] Significantly different from the same genotype fed normal chow ($P < 0.05$).

$ATM^{+/+}/LDLR^{-/-}$ mice, respectively, under normal chow or a high-fat diet. These data suggest that a heterozygous *ATM* mutation selectively increases the severity of hypercholesterolemia among *ApoE*-deficient mice.

Plasma clearance of apoB-48-carrying lipoproteins

To investigate whether the increased plasma apoB-48-carrying lipoproteins in the $ATM^{+/-}/ApoE^{-/-}$ mice resulted from a reduced clearance of these proteins, we determined the clearance of ^{125}I-labeled apoB-48-carrying lipoproteins from the circulation. **Figure 3A** shows that the clearance of apoB-48-carrying lipoproteins is reduced significantly among the $ATM^{+/-}/ApoE^{-/-}$ mice compared with that of the $ATM^{+/+}/ApoE^{-/-}$ controls. For example, ~53% of injected apoB-48-carrying lipoproteins were cleared from the plasma of the $ATM^{+/+}/ApoE^{-/-}$ mice within 4 h, whereas only ~38% of the injected dose was cleared in the $ATM^{+/-}/ApoE^{-/-}$ mice during the same period. Figure 3B shows the hepatic uptake of apoB-48-carrying lipoproteins. At 4 h after injection of ^{125}I-labeled apoB-48-carrying lipoproteins, ~29% of the injected radioactivity was recovered from the livers of the $ATM^{+/+}/ApoE^{-/-}$ mice, but only ~20% was recovered from the livers of $ATM^{+/-}/ApoE^{-/-}$ mice. These data suggest that the severe hypercholesterolemia of $ATM^{+/-}/ApoE^{-/-}$ mice comes mainly from a reduced clearance of plasma apoB-48-carrying lipoproteins and that the reduced uptake of blood-circulating apoB-48-carrying lipoproteins by liver cells is, at least partially, responsible for the reduction in the clearance of these lipoproteins.

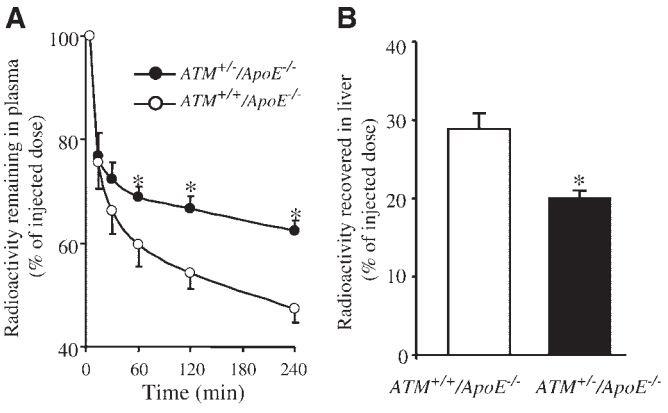

Fig. 3. Clearance of apoB-48-carrying lipoproteins. ^{125}I-labeled apoB-48-carrying lipoproteins were injected into $ATM^{+/-}/ApoE^{-/-}$ and $ATM^{+/+}/ApoE^{-/-}$ mice via the tail vein. Blood samples were collected at various time points, and the liver was collected after the last blood sampling. The radioactivity in the plasma and liver was measured as described in Materials and Methods. The presence of apoB-48-carrying lipoproteins in the plasma (A) and liver (B) is presented as the percentage of the injected dose. Values represent means ± SEM of five mice. * Significantly different from $ATM^{+/+}/ApoE^{-/-}$ mice ($P < 0.05$).

Hepatic secretion of apoB and triglycerides

To investigate whether the increased plasma cholesterol levels in the $ATM^{+/-}/ApoE^{-/-}$ mice were related to an enhanced hepatic secretion of VLDL, mice were injected with Triton WR1339, which blocked the catabolism of plasma VLDL. Under these circumstances, the time-related increase in plasma apoB and triglycerides is directly related to hepatic VLDL secretion. As shown in **Fig. 4A**, **B**, the level of plasma apoB-100 increased after the Triton injections, the increased magnitude over time was similar among the $ATM^{+/+}/ApoE^{-/-}$ and $ATM^{+/-}/ApoE^{-/-}$ mice, and no significant increase in plasma apoB-48 was observed in either the $ATM^{+/+}/ApoE^{-/-}$ or $ATM^{+/-}/ApoE^{-/-}$ mice in-

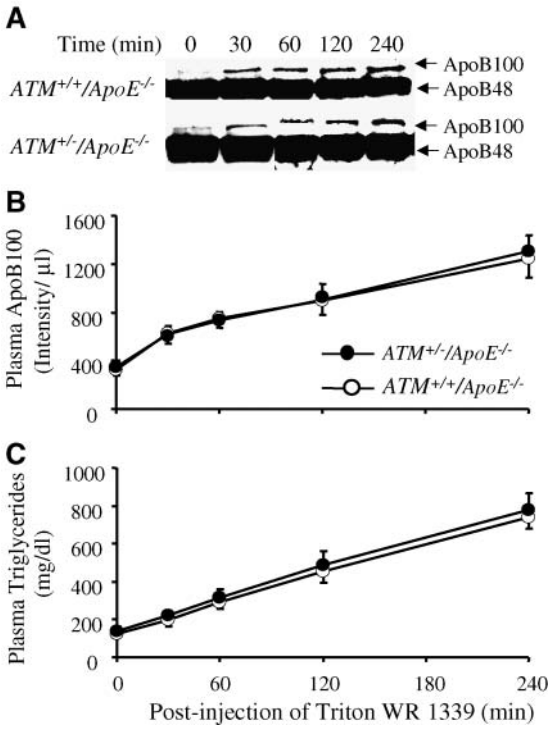

Fig. 4. Hepatic secretion of apoB-carrying lipoproteins. Triton WR1339 was injected into $ATM^{+/-}/ApoE^{-/-}$ and $ATM^{+/+}/ApoE^{-/-}$ mice via the tail vein, and blood samples were collected at various time points. Plasma apoB was measured with Western blot analysis. A: Representative Western blots of apoB. B: The level of plasma apoB-100 is expressed as the relative intensity of the immunoblots. C: Plasma triglycerides were measured with a colorimetric assay as described in Materials and Methods. Values represent means ± SEM of five mice.

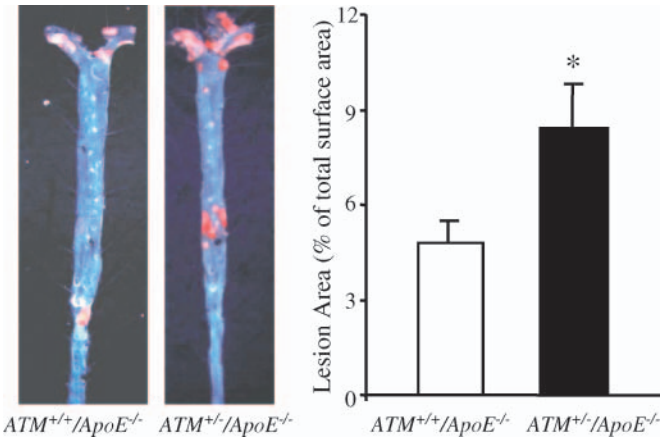

Fig. 5. Quantitation of atherosclerosis in the en face preparation of mouse aortas. $ATM^{+/-}/ApoE^{-/-}$ and $ATM^{+/+}/ApoE^{-/-}$ mice were killed at 14 weeks of age. Atherosclerotic lesions in the en face mouse aortas were examined by Sudan IV staining. The area of atherosclerotic lesions and the area of the aortic surface were measured as described in Materials and Methods. Data are expressed as percentages of surface area of the aorta covered by atherosclerotic lesions. Values are means ± SEM of 10 mice for each group. * Significantly different from $ATM^{+/+}/ApoE^{-/-}$ mice ($P < 0.05$).

jected with Triton WR1339 (Fig. 4A). Figure 4C shows that plasma triglycerides were increased after the Triton injections; however, the mean level of plasma triglycerides was equivalent between the $ATM^{+/+}/ApoE^{-/-}$ and $ATM^{+/-}/ApoE^{-/-}$ mice at all time points studied. These results suggest that superimposition of a heterozygous *ATM* mutation onto an *ApoE* deficiency background does not significantly affect hepatic VLDL production in mice.

Aortic atherosclerosis

The atherosclerotic lesions seen in the aorta of the $ATM^{+/-}/ApoE^{-/-}$ and $ATM^{+/+}/ApoE^{-/-}$ mice fed a normal chow diet were first analyzed by en face lipid staining. At 14 weeks of age, the atherosclerotic lesions occurred mostly at the proximal aorta. The lesion area observed in the $ATM^{+/-}/ApoE^{-/-}$ mice was significantly larger than that observed in the $ATM^{+/+}/ApoE^{-/-}$ mice (**Fig. 5**). Approximately 8.4% of the aortic surface area was affected by atherosclerotic lesions in the $ATM^{+/-}/ApoE^{-/-}$ mice, whereas only 4.7% of the aorta surface was affected by atherosclerosis in the $ATM^{+/+}/ApoE^{-/-}$ mice (Fig. 5). Histopathological examination using light microscopy also showed that the size of the atherosclerotic lesions in the aortic sinus of the $ATM^{+/-}/ApoE^{-/-}$ mice was significantly larger than that in the $ATM^{+/+}/ApoE^{-/-}$ controls (**Table 3**). In addition, the histological features of the atherosclerotic lesions in the $ATM^{+/-}/ApoE^{-/-}$ mice differed from those of the $ATM^{+/+}/ApoE^{-/-}$ mice. All of the $ATM^{+/-}/ApoE^{-/-}$ mice developed both early stage (e.g., foam cells and free lipids) and later stage (e.g., fibrous caps and acellular areas) lesions. In contrast, only approximately half of the $ATM^{+/+}/ApoE^{-/-}$ mice showed fibrous caps and acellular areas in the atherosclerotic lesions located in the mouse aortic sinus (Table 3). This atherogenic effect of the heterozygous *ATM* mutation was specific for $ApoE^{-/-}$ mice, because we did not observe any significant differences between the $ATM^{+/-}/LDLR^{-/-}$ and the $ATM^{+/+}/LDLR^{-/-}$ mice with respect to lesion size and the histopathology in the aorta (data not shown).

DISCUSSION

This report clearly demonstrates that the $ATM^{+/-}/ApoE^{-/-}$ mice suffered severe hypercholesterolemia compared with their $ATM^{+/+}/ApoE^{-/-}$ littermates, whereas the plasma cholesterol levels in the $ATM^{+/-}$ and $ATM^{+/-}/LDLR^{-/-}$ mice were only slightly higher than those of their controls under normal chow or a high-fat diet. FPLC analysis revealed that the increased cholesterol levels observed among the $ATM^{+/-}/ApoE^{-/-}$ mice were distributed primarily in the VLDL and LDL fractions. In addition, the level of plasma apoB-48 in the $ATM^{+/-}/ApoE^{-/-}$ mice was significantly higher than in the $ATM^{+/+}/ApoE^{-/-}$ mice. These data suggest that overaccumulation of apoB-48-carrying lipoproteins contributes to the severe hypercholesterolemia observed among the $ATM^{+/-}/ApoE^{-/-}$ mice. This overaccumulation of lipoproteins cannot be explained by an increased influx of chylomicrons or VLDLs into the bloodstream, because the $ATM^{+/-}/ApoE^{-/-}$ and $ATM^{+/+}/ApoE^{-/-}$ mice showed comparable levels of food consumption (data not shown) and hepatic secretion of triglycerides and apoB-100. However, our data are consistent with the interpretation that the overaccumulation of apoB-48-carrying lipoproteins in the $ATM^{+/-}/ApoE^{-/-}$ mice results mainly from a reduced removal of chylomicron remnants from the blood circulation, because the

TABLE 3. Atherosclerotic lesions in the mouse aorta sinus

Mouse	Lesion Size	Foam Cells	Free Lipids	Acellular Areas	Fibrous Caps	Calcification
	$10^3\ \mu m^2$					
$ATM^{+/+}/ApoE^{-/-}$	34.6 ± 5.3	20/20	20/20	7/20	12/20	3/20
$ATM^{+/-}/ApoE^{-/-}$	61.5 ± 8.1[a]	20/20	20/20	16/20	20/20	12/20

Sequential 8 μm thick sections were cut from the aortic sinus of $ATM^{+/-}/ApoE^{-/-}$ and $ATM^{+/+}/ApoE^{-/-}$ mice at 14 weeks of age. Sections were stained with Oil Red O. The area (μm^2) of atherosclerotic lesions in the section was measured. Data are expressed as means ± SEM of 20 mice for each group. The histological features (e.g., foam cells, free lipids, fibrous caps, acellular areas, and calcifications) were also measured. Those data are expressed as number of mice with characteristic features/total number of mice studied.

[a] Significantly different from $ATM^{+/+}/ApoE^{-/-}$ mice ($P < 0.05$).

ATM$^{+/-}$/*ApoE*$^{-/-}$ mice had a significantly reduced clearance of plasma apoB-48-carrying lipoproteins compared with the *ATM*$^{+/+}$/*ApoE*$^{-/-}$ mice.

Currently, the mechanism underlying the reduced clearance of plasma apoB-48-carrying lipoproteins in *ATM*$^{+/-}$/*ApoE*$^{-/-}$ mice has not been defined. However, it is interesting that several proposed functions of ATM in the cytoplasm, if lost or reduced, could impair the uptake of lipoproteins. For example, the ATM protein has been suggested to play a role in signaling transduction (19, 20). Cells lacking ATM have been shown to be defective in intracellular Ca^{2+} mobilization and phosphatidylinositol 3-kinase activation (19). Phosphatidylinositol-3-phosphate, which is abundant in endosomes, has been suggested to play a critical role in vesicle transport (21). Interestingly, cells lacking ATM have been shown to accumulate uncharacterized lipid cytosomes and lysosomes (22). In addition, the ATM protein has been shown to interact with β-adaptin (20), a component of the adaptor protein complex-2, which recruits soluble clathrin to the plasma membrane to form the clathrin coat. The clathrin-coated pit is a plasma membrane microdomain that mediates the receptor-related internalization of molecules from the cell surface (for review, see 21). Thus, it is highly likely that the ATM protein participates in the endocytic process via its kinase activity to regulate the proteins and/or lipids that manage clathrin-coated pit formation and vesicle transport. Of interest, our data demonstrate that severe hypercholesterolemia occurs only when a heterozygous *ATM* mutation combines with a null *ApoE* mutation, suggesting that the endocytic pathway, in which ATM plays a part, does not need apoE.

Under physiological conditions, apoE, by binding to cell surface LDLR and LDLR-related protein (LRP), initiates receptor-mediated endocytosis (for review, see 23). In the absence of apoE, the remnants of the apoB-100-carrying lipoproteins (e.g., LDL) can still be absorbed by liver cells through the apoB-100-LDLR interaction. However, chylomicron remnants that carry apoB-48 do not have a ligand for the LDLR or LRP and therefore cannot be internalized via the endocytic pathway mediated by these receptors. It is notable, however, that the hypercholesterolemia observed among the *ApoE*-deficient mice fed a normal chow diet is maintained within narrow limits (between 400 and 600 mg/dl), despite the continuous generation of apoB-48-carrying remnants from the chylomicrons (12, 15). Apparently, in the absence of apoE, there are other pathways that can mediate the removal of apoB-48-carrying remnants from the circulation, albeit not as efficiently as the apoE-mediated process. The development of severe hypercholesterolemia in the *ATM*$^{+/-}$/*ApoE*$^{-/-}$ mice, but not in the *ATM*$^{+/-}$ or the *ATM*$^{+/-}$/*LDLR*$^{-/-}$ mice, suggests that ATM plays a role in such apoE-independent pathway(s) for the catabolism of apoB-48-carrying remnants.

Previous studies have shown apoE-independent mechanisms that mediate the uptake of lipoprotein remnants. For example, Magoori et al. (24) reported that mice with double deficiencies in apoE and LRP-5 displayed severe hypercholesterolemia compared with mice lacking apoE alone and that this hypercholesterolemia resulted mainly from an increased level of apoB-48-carrying remnants in the plasma (24). However, a deficiency of LRP-5 alone had no significant effect on the plasma cholesterol level. These results suggest that LRP-5 mediates an apoE-independent catabolism of plasma lipoprotein remnants. One possible mechanism by which the ATM protein contributes to the catabolism of apoB-48-carrying lipoproteins might be related to the LRP-5-mediated endocytic pathway. It is likely that the interaction of apoB-48-carrying lipoproteins with membrane receptors, such as LRP-5, may activate the cytoplasmic ATM via an unknown mechanism, and the activated ATM in turn regulates the endocytosis of apoB-48-carrying lipoproteins through the phosphorylation of proteins such as β-adaptin and/or lipids such as phosphatidylinositol-3.

Another important observation in this report is that the *ATM*$^{+/-}$/*ApoE*$^{-/-}$ mice suffered severe atherosclerotic lesions compared with their *ATM*$^{+/+}$/*ApoE*$^{-/-}$ littermates, whereas the intensity of atherosclerosis in the *ATM*$^{+/-}$ and *ATM*$^{+/-}$/*LDLR*$^{-/-}$ mice fed normal chow or high-fat diets was comparable to that of their controls (data not shown). These findings are not surprising because the development of atherosclerotic lesions in *ApoE*$^{-/-}$ mice is known to be accelerated when the level of apoB-48-carrying remnants in the circulation is increased [e.g., when these mice are fed a high-fat diet (25) or imposed on a LRP-5 deficiency (24)]. Therefore, the overaccumulation of apoB-48-carrying remnants in the plasma of *ATM*$^{+/-}$/*ApoE*$^{-/-}$ mice not surprisingly leads to the development of severe atherosclerotic lesions.

In summary, the results presented here demonstrate for the first time that a heterozygous mutation in the *ATM* gene causes an overaccumulation of plasma apoB-48-carrying lipoproteins and, consequently, a rapid development of atherosclerotic lesions in apoE-deficient mice. Our data also demonstrate that the overaccumulation of plasma apoB-48-carrying lipoproteins in these mice results mainly from a reduced removal of blood-circulating apoB-48-carrying lipoproteins. Moreover, we observed that severe hypercholesterolemia occurred only with a combination of a heterozygous *ATM* mutation and a null *ApoE* mutation, but not in the heterozygous *ATM* mutation alone or in the combined heterozygous *ATM* and null *LDLR* mutations. These observations suggest that ATM is involved in an apoE-independent pathway to facilitate the catabolism of apoB-48-carrying remnants. Findings from this report might be clinically important because a heterozygous mutation at the *ATM* locus in humans might increase the risk of ischemic heart disease (6) and because heterozygous *ATM* carriers have been estimated to constitute ~1–2% of the general population (6).

The authors thank Dr. Lee E. Limbird, Dr. Sergio Fazio and Dr. MacRae F. Linton for critically reading the manuscript and their useful suggestions. This study was supported by American Heart Association Award 0030239N (Z.G.) and by National Institutes of Health Grants GM-08037 (Z.G.) and HL-076623 (H.Y.).

REFERENCES

1. Rotman, G., and Y. Shiloh. 1998. ATM: from gene to function. *Hum. Mol. Genet.* **7:** 1555–1563.
2. Watters, D., P. Kedar, K. Spring, J. Bjorkman, P. Chen, M. Gatei, G. Birrell, B. Garrone, P. Srinivasa, D. I. Crane, et al. 1999. Localization of a portion of extranuclear ATM to peroxisomes. *J. Biol. Chem.* **274:** 34277–34282.
3. Gatti, R. A., E. Boder, H. V. Vinters, R. S. Sparkes, A. Norman, and K. Lange. 1991. Ataxia-telangiectasia: an interdisciplinary approach to pathogenesis. *Medicine.* **70:** 99–117.
4. Meyn, M. S. 1995. Ataxia-telangiectasia and cellular responses to DNA damage. *Cancer Res.* **55:** 5991–6001.
5. Swift, M. 1985. Genetics and epidemiology of ataxia-telangiectasia. *Kroc Found. Ser.* **19:** 133–146.
6. Swift, M., and C. Chase. 1983. Cancer and cardiac death in obligatory ataxia-telangiectasia. *Lancet.* **1:** 1049–1050.
7. Badalian, L. O., and L. V. Kalinina. 1976. Lipid metabolism disorder in ataxia-telangiectasia. *Zh. Nevropatol. Psikhiatrii Im.* **76:** 655–659.
8. Barlow, C., S. Hirotsune, R. Paylor, M. Liyanage, M. Eckhaus, F. Collins, Y. Shiloh, J. N. Crawley, T. Ried, D. Tagle, et al. 1996. *Atm*-deficient mice: a paradigm of ataxia telangiectasia. *Cell.* **86:** 159–171.
9. Elson, A., Y. Wang, C. J. Daugherty, C. C. Morton, F. Zhou, J. Campos-Torres, and P. Leder. 1996. Pleiotropic defects in ataxia-telangiectasia protein-deficient mice. *Proc. Natl. Acad. Sci. USA.* **93:** 13084–13089.
10. Worgul, B. V., L. Smilenov, D. J. Brenner, A. Junk, W. Zhou, and E. J. Hall. 2002. Atm heterozygous mice are more sensitive to radiation-induced cataracts that are their wild-type counterparts. *Proc. Natl. Acad. Sci. USA.* **99:** 9836–9839.
11. Smilenov, L. B., D. J. Brenner, and E. J. Hall. 2001. Modest increased sensitivity to radiation oncogenesis in ATM heterozygous versus wild-type mammalian mice. *Cancer Res.* **61:** 5710–5713.
12. Piedrahita, J. A., S. H. Zhang, J. R. Hagaman, P. M. Oliver, and N. Maeda. 1992. Generation of mice carrying a mutant apolipoprotein E gene inactivated by gene targeting in embryonic stem cells. *Proc. Natl. Acad. Sci. USA.* **89:** 4471–4475.
13. Ishibashi, S., J. L. Goldstein, M. S. Brown, J. Herz, and D. K. Burns. 1994. Massive xanthomatosis and atherosclerosis in cholesterol-fed low density lipoprotein receptor-negative mice. *J. Clin. Invest.* **93:** 1885–1893.
14. Farese, R. V., Jr., M. M. Veniant, C. M. Cham, L. M. Flynn, V. Pierotti, J. F. Loring, M. Traber, S. Ruland, R. S. Stokowski, D. Huszar, et al. 1996. Phenotypic analysis of mice expressing exclusively apolipoprotein B48 or apolipoprotein B100. *Proc. Natl. Acad. Sci. USA.* **93:** 6393–6398.
15. Guo, Z. M., F. Mitchell-Raymundo, H. Yang, Y. Ikeno, J. Nelson, V. Diaz, A. Richardson, and R. Reddick. 2002. Dietary restriction reduces atherosclerosis and oxidative stress in the aorta of apolipoprotein E-deficient mice. *Mech. Ageing Dev.* **123:** 1121–1131.
16. Hasty, A. H., M. F. Linton, L. L. Swift, and S. Fazio. 1999. Determination of lower threshold of apolipoprotein E resulting in remnant lipoprotein clearance. *J. Lipid Res.* **40:** 1529–1538.
17. Mindham, M. A., and P. A. Mayes. 1992. A simple and rapid method for the preparation of apolipoproteins. *Electrophoresis.* **16:** 998–1001.
18. Sobal, G., U. Resch, and H. Sinzinger. 2004. Modification of low-density lipoprotein by different radioiodination methods. *Nucl. Med. Biol.* **31:** 381–388.
19. Grimmer, G., W. Stober, J. Jacob, U. Mohr, K. Schoene, H. Brune, and J. Misfeld. 1983. Inventory and biological impact of polycyclic carcinogens in the environment. *Exp. Pathol.* **24:** 3–13.
20. Lim, D. S., D. G. Kirsch, C. E. Canman, J. H. Ahn, Y. Ziv, L. S. Newman, R. B. Darnell, Y. Shiloh, and M. B. Kastan. 1998. ATM binds to beta-adaptin in cytoplasmic vesicles. *Proc. Natl. Acad. Sci. USA.* **95:** 10146–10151.
21. Schroeder, F., A. M. Gallegos, B. P. Atshaves, S. M. Storey, A. L. McIntosh, A. D. Petrescu, H. Huang, O. Starodub, H. Chao, H. Yang, et al. 2001. Recent advances in membrane microdomains: rafts, caveolae, and intracellular cholesterol trafficking. *Exp. Biol. Med. (Maywood).* **226:** 873–890.
22. Barlow, C., C. Ribaut-Barassin, T. A. Zwingman, A. J. Pope, K. D. Brown, J. W. Owens, D. Larson, E. A. Harrington, A-M. Haeberle, J. Mariani, et al. 2000. ATM is a cytoplasmic protein in mouse brain required to prevent lysosomal accumulation. *Proc. Natl. Acad. Sci. USA.* **97:** 871–876.
23. Havel, R. J., and R. L. Hamilton. 2004. Hepatic catabolism of remnant lipoproteins: where the action is. *Arterioscler. Thromb. Vasc. Biol.* **24:** 213–215.
24. Magoori, K., M-J. Kang, M. R. Ito, H. Kakunch, R. X. Ioka, A. Kamataki, D-H. Kim, H. Asaba, S. Iwasaki, Y. A. Takei, et al. 2003. Severe hypercholesterolemia, impaired fat tolerance, and advanced atherosclerosis in mice lacking both low density lipoprotein receptor-related protein 5 and apolipoprotein E. *J. Biol. Chem.* **278:** 11331–11336.
25. Ishibashi, S., J. Herz, N. Maeda, J. L. Goldstein, and M. S. Brown. 1994. The two-receptor model of lipoprotein clearance: tests of the hypothesis in "knockout" mice lacking the low density lipoprotein receptor, apolipoprotein E, or both proteins. *Proc. Natl. Acad. Sci. USA.* **91:** 4431–4435.

ERRATA

In the article "Heterozygous mutation of ataxia-telangiectasia mutated gene aggravates hypercholesterolemia in apoE-deficient mice" by Wu et al., published in the July 2005 issue of the *Journal of Lipid Research* (Volume **46**, pages 1380–1387), the correct spelling of the name of one of the coauthors is: George Jules.

The Instructions to Authors for the *Journal of Lipid Research* are online at http://www.jlr.org/misc/ifora.shtml